IOP Publishing New J. Phys. 26 (2024) 083015 https://doi.org/10.1088/1367-2630/ad6bb7

New Journal of Physics
The open access journal at the forefront of physics

Deutsche Physikalische Gesellschaft DPG
IOP Institute of Physics

Published in partnership with: Deutsche Physikalische Gesellschaft and the Institute of Physics

OPEN ACCESS

RECEIVED
24 May 2024

REVISED
19 July 2024

ACCEPTED FOR PUBLICATION
6 August 2024

PUBLISHED
14 August 2024

PAPER

Theoretical concept of error-rejecting entanglement purification of quantum-dots electronic spins in single-sided optical microcavity

Jingyao Wang[1] **and Xin Wang**[2,*]

[1] Key Laboratory for Microstructural Material Physics of Hebei Province, School of Science, Yanshan University, Qinhuangdao 066004, People's Republic of China
[2] Center for Advanced Quantum Studies, Department of Physics, Beijing Normal University, Beijing 100875, People's Republic of China
[*] Author to whom any correspondence should be addressed.

E-mail: xinwang17@mail.bnu.edu.cn

Abstract

We use the quantum-dots (QD) coupled with single-sided microcavities system to construct the error-rejecting controlled not (CNOT) gate of electronic spins system in QD; We have designed an error-rejecting entanglement purification protocol (EPP) of electronic spins system in QD by using the error-rejecting CNOT gate and unitary operation. It can extract the high entanglement from the mixed entanglement states of the electronic spins with low entangled states. This EPP can eliminate the operation errors caused by the nonideal interaction between photons and QD coupled with optical microcavities system, and improve the fidelity of the EPP through iteration. Our scheme is more practical in future long-distance quantum communications, especially providing significant benefits for solving decoherence problems in quantum networks and quantum repeaters.

1. Introduction

Quantum communication is an innovative and secure method for transmitting information [1]. It relies heavily on quantum entanglement, which plays a crucial role in various protocols such as quantum teleportation [2], quantum dense coding (QDC) [3, 4], quantum key distribution (QKD) [5–8], quantum secret sharing (QSS) [9], and quantum secure direct communication (QSDC) [10, 11]. However, channel noise presents a significant challenge, limiting the range of entanglement distribution by inducing decoherence over long distances [12,13]. To overcome this, quantum repeaters [12–14] serve as an efficient solution, mitigating decoherence resulting from noise-induced destructive effects [15]. Within a quantum repeater protocol, entanglement distillation, which includes entanglement purification protocol (EPP) [16] and entanglement concentration protocol (ECP) [17], plays a critical role. Here, we focus on discussing EPP.

EPP involves distilling high-quality entangled states from low-quality mixed entangled states. In 1996, Bennett *et al* [16] first utilized CNOT gates to achieve entanglement purification of Werner states. Later that year, Deutch *et al* [18] improved upon Bennett *et al*'s EPP. In 2001, Pan *et al* [19] proposed a theoretical scheme for photon polarization entanglement purification using linear optical elements and ideal entangled sources. In 2003, Pan *et al* [20] experimentally implemented an EPP based on linear optical elements using parametric down-conversion (PDC) entangled sources. In 2006, Reichle *et al* [21] experimentally achieved EPP of atoms. In 2008, Sheng *et al* [22] introduced an EPP based on quantum nondemolition detectors (QND) using nonlinear cross-Kerr media, which can be iteratively employed. In 2010, Sheng *et al* [23] proposed a deterministic EPP based on nonlinear cross-Kerr media. This scheme achieves deterministic entanglement purification by consuming spatial and frequency entanglement in two separate steps without disrupting any entangled photon pairs. In the same year, Sheng *et al* [24] proposed a deterministic EPP based on PDC entangled sources. This scheme requires only one unitary operation to obtain maximally entangled photon pairs. In 2011, Deng [25] introduced a multiparticle EPP capable of deterministic entanglement purification of N-photon Greenberger–Horne–Zeilinger (GHZ) states. This scheme extends the concept of deterministic entanglement purification to multi-photon systems. In the same year, Wang *et al* [26] proposed an EPP for entangled electron pairs using QD-coupled optical microcavity systems. This scheme is

implemented using parity detection gates. In 2020, Lu *et al* [27] proposed a universal EPP using controlled-phase gates in QD-coupled bilateral cavity systems. Also in the same year, Lu *et al* [28] introduced a predictable EPP based on diamond NV center-coupled single-sided optical microcavity systems. This scheme utilizes the predictive function of parity detection gates to filter out errors caused by non-ideal interactions between photons and diamond NV center-coupled single-sided optical microcavity systems. In 2020, Cao *et al* [29] introduced a method for analyzing Hyperentangled-Bell states in two-photon hyperentangled systems using QDs coupled with double-sided microcavities. Building on this, in 2022, Yin *et al* [30] presented an EPP utilizing QDs coupled with double-sided microcavities, along with nondestructive parity-check detectors (PCDs). These advancements underscore the growing potential of QDs in enabling advanced quantum communication and information processing protocols.

In this paper, we achieve error-rejecting EPP of QD electronic spins by employing unitary operations and constructing error-rejecting CNOT gates to purify high-quality entangled states from low-quality mixed entangled states. However, imperfections in the input-output relations during the interaction between photons and the system in QD-coupled single-sided optical microcavity systems can degrade the fidelity of EPP. Leveraging error-rejecting CNOT gates for QD electronic spins enables us to convert the factors that degrade fidelity into detectable operational errors, thereby circumventing the fidelity degradation caused by non-ideal interactions.

2. The system

Now let us discuss a quantum system: embedding In(Ga)As self-assembled QD into a single-sided optical microcavity [31–34], as depicted in figure 1. Both sides of the pillar microcavity are formed with Bragg reflectors. The top reflector is partially reflective. Placing a single QD at the antinode of a pillar microcavity, injecting additional electrons into the QD, and optically exciting to form a negative trion X^- (composed of two electrons and one hole). The cavity axis z is selected along the growth direction of the QD and parallel to the propagation direction of the photons, shown in figure 1(b). The electronic ground state is represented as $|\uparrow\rangle$ and $|\downarrow\rangle$, with their projections on the z-axis being $\left|+\frac{1}{2}\right\rangle$ and $\left|-\frac{1}{2}\right\rangle$ respectively. The spin states of the negative trion can be represented as $|\uparrow\downarrow\Uparrow\rangle$ and $|\downarrow\uparrow\Downarrow\rangle$, with their projections on the z-axis being $\left|+\frac{3}{2}\right\rangle$ and $\left|-\frac{3}{2}\right\rangle$ respectively. The dipole transition associated with the negatively charged QD is strictly governed by Pauli's exclusion principle [35], shown in figure 1(a). The dipole-allowed transitions between the ground state and the trion state are $|\uparrow\rangle \leftrightarrow |\uparrow\downarrow\Uparrow\rangle$ and $|\downarrow\rangle \leftrightarrow |\uparrow\downarrow\Downarrow\rangle$, along with the absorption of a right-handed circularly polarized photon ($|R\rangle$) and a left-handed one ($|L\rangle$), respectively, while the crossing transitions are dipole forbidden [35].

The circularly polarized probe photon injected into the single-sided optical microcavity undergo reflection by the cavity, with a reflection coefficient $r_j(\omega)$ [31–34]. This dynamic process can be described by the Heisenberg equations of motion for the cavity field operator $\hat{a}$ and the dipole operator $\hat{\sigma}_-$ in the interaction picture [36],

$$\begin{aligned}\frac{\mathrm{d}\hat{a}}{\mathrm{d}t} &= -\left[i(\omega_c-\omega)+\frac{\kappa}{2}+\frac{\kappa_s}{2}\right]\hat{a}-g\hat{\sigma}_- -\sqrt{\kappa}\hat{a_{\mathrm{in}}}+\hat{R},\\ \frac{\mathrm{d}\hat{\sigma}_-}{\mathrm{d}t} &= -\left[i(\omega_{X^-}-\omega)+\frac{\gamma}{2}\right]\hat{\sigma}_- -g\hat{\sigma}_z\hat{a}+\hat{N}.\end{aligned} \tag{1}$$

In this scenario, ω represents the frequency of the probe photon, while ω_c denotes the frequency of the cavity mode. g represents the coupling strength between X^- and the cavity mode. $\frac{\kappa}{2}$ and $\frac{\kappa_s}{2}$ are the decay rate and leakage rate of the single-sided optical microcavity, respectively. $\frac{\gamma}{2}$ is the decay rate of the negative trion. $\hat{R}$ and $\hat{N}$ are noise operators. The input field operator $\hat{a}_{\mathrm{in}}$ and the output field operator $\hat{a}_{\mathrm{out}}$ satisfy the boundary condition $\hat{a}_{\mathrm{out}}=\hat{a}_{\mathrm{in}}+\sqrt{\kappa}\hat{a}$ [36]. Under the weak excitation condition, the reflection coefficient can be expressed as [32, 33, 37]:

$$r_j(\omega)=1-\frac{\kappa\left[i(\omega_{X^-}-\omega)+\frac{\gamma}{2}\right]}{\left[i(\omega_{X^-}-\omega)+\frac{\gamma}{2}\right]\left[i(\omega_c-\omega)+\frac{\kappa}{2}+\frac{\kappa_s}{2}\right]+jg^2}. \tag{2}$$

The subscript j is used to distinguish the QD-cavity coupled system and the empty cavity. When the polarized probe photon aligns with the trion transition, the system forms a QD-cavity coupled system ($j=1$). Moreover, when the polarized photon decouples from the trion transition, the cavity remains empty ($j=0$)[38, 39]

$$\begin{aligned}|R\rangle|\uparrow\rangle &\rightarrow r_1|R\rangle|\uparrow\rangle, \quad |R\rangle|\downarrow\rangle \rightarrow r_0|R\rangle|\downarrow\rangle,\\ |L\rangle|\uparrow\rangle &\rightarrow r_0|L\rangle|\uparrow\rangle, \quad |L\rangle|\downarrow\rangle \rightarrow r_1|L\rangle|\downarrow\rangle.\end{aligned} \tag{3}$$

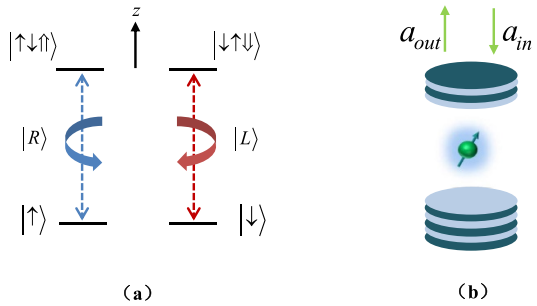

Figure 1. The spin-dependent transitions for negatively charged exciton X^{-}. (a) The relative energy levels and the optical transitions of a QD. (b) A singly charged QD inside a single-sided optical microcavity.

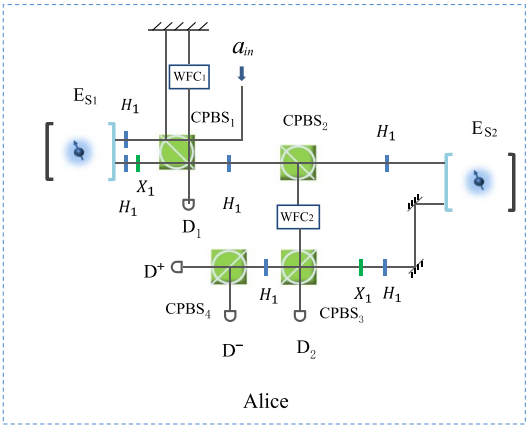

Figure 2. The schematic diagram of error rejecting CNOT gate.

Based on the interaction between photon and electronic spins in the QD-coupled single-sided optical microcavity system introduced earlier, we have constructed an error-rejecting CNOT gate for QD electronic spins, as illustrated in figure 2. The error-rejecting CNOT gate consists of two QD-coupled optical microcavity systems, four circularly polarizing beam splitters (CPBSs), two individual half-wave-plates (HWP) X_1, six components H_1, four single-photon detectors, three plane mirrors, and two waveform correctors (WFC). The optical axis of HWP X_1 is oriented at 0° with respect to the horizontal polarization direction, allowing for bit-flip operations on circularly polarized photon, $|R\rangle \leftrightarrow |L\rangle$. The component H_1 (comprised of a sequence of components including a HWP at 0°, a quarter-wave-plates (QWP) at 0°, a HWP at 22.5°, and a QWP at 0°) performs Hadamard operations [27] on circularly polarized photon, $|R\rangle \rightarrow \frac{1}{\sqrt{2}}(|R\rangle + |L\rangle), |L\rangle \rightarrow \frac{1}{\sqrt{2}}(|R\rangle - |L\rangle)$.

The electronic spins in the QD-coupled single-sided optical microcavity systems E_{S_1} and E_{S_2} are denoted as S_1 and S_2, respectively. Assuming the initial state of the incoming photon is $|\varphi\rangle_a = \frac{1}{\sqrt{2}}(|R\rangle + |L\rangle)$, and the initial states of the electronic spins S_1 and S_2 are $|\varphi_{s1}\rangle = \alpha_1|\uparrow\rangle + \beta_1|\downarrow\rangle$ and $|\varphi_{s2}\rangle = \alpha_2|\uparrow\rangle + \beta_2|\downarrow\rangle$. The initial state of the composite system formed by photon a and electronic spins S_1S_2 is:

$$|\varphi_1\rangle = \frac{1}{\sqrt{2}}(|R\rangle + |L\rangle)(\alpha_1|\uparrow\rangle + \beta_1|\downarrow\rangle)(\alpha_2|\uparrow\rangle + \beta_2|\downarrow\rangle). \tag{4}$$

The photon first passes through $CPBS_1$, where right-circularly polarized photon $|R\rangle$ is transmitted, and left-circularly polarized light $|L\rangle$ is reflected. Afterwards, the photon passes through component H_1 (performing a Hadamard operation on the photon). Subsequently, the photon a interacts with QD-coupled optical microcavity system E_{S_1}. Then the photon passes through H_1. The state of the composite system of photon a and electronic spins S_1S_2 evolves to

$$|\varphi_2\rangle = \frac{1}{2\sqrt{2}}|R\rangle(r_1+r_0)(\alpha_1|\uparrow\rangle+\beta_1|\downarrow\rangle)(\alpha_2|\uparrow\rangle+\beta_2|\downarrow\rangle) + \frac{1}{2\sqrt{2}}|L\rangle(r_1-r_0)(\alpha_1|\uparrow\rangle-\beta_1|\downarrow\rangle)(\alpha_2|\uparrow\rangle+\beta_2|\downarrow\rangle) + \frac{1}{\sqrt{2}}|L\rangle(\alpha_1|\uparrow\rangle+\beta_1|\downarrow\rangle)(\alpha_2|\uparrow\rangle+\beta_2|\downarrow\rangle). \quad (5)$$

After passing through X_1 to perform a bit-flip operation on the $|R\rangle$ component of the incoming photon, while the $|L\rangle$ component, after being reflected by $CPBS_1$ and then by a plane mirror, passes through a $WFC_1(|i\rangle \rightarrow \frac{1}{2}(r_1-r_0)|i\rangle)$, the state of the composite system of photon a and electronic spins S_1S_2 evolves to

$$|\varphi_3\rangle = \frac{1}{2\sqrt{2}}|L\rangle(r_1+r_0)(\alpha_1|\uparrow\rangle+\beta_1|\downarrow\rangle)(\alpha_2|\uparrow\rangle+\beta_2|\downarrow\rangle) + \frac{1}{2\sqrt{2}}|R\rangle(r_1-r_0)(\alpha_1|\uparrow\rangle-\beta_1|\downarrow\rangle)(\alpha_2|\uparrow\rangle+\beta_2|\downarrow\rangle) + \frac{1}{2\sqrt{2}}|L\rangle(r_1-r_0)(\alpha_1|\uparrow\rangle+\beta_1|\downarrow\rangle)(\alpha_2|\uparrow\rangle+\beta_2|\downarrow\rangle). \quad (6)$$

The first term on the right side of equation (6) triggers detector D_1 response, $|\phi_1\rangle = \frac{1}{2\sqrt{2}}|L\rangle(r_1+r_0)(\alpha_1|\uparrow\rangle+\beta_1|\downarrow\rangle)(\alpha_2|\uparrow\rangle+\beta_2|\downarrow\rangle)$. If detector D_1 does not respond, the photon passes through component H_1 (perform a Hadamard operation on circularly polarized photon). Then we need to perform a Hadamard operation on the electronic spin S_2 before passing through $CPBS_2$. After passing through $CPBS_2$, where $|R\rangle$ is transmitted and $|L\rangle$ is reflected, $|R\rangle$ then passes through H_1. Subsequently, the photon a interacts with the QD-coupled single-sided optical microcavity system E_{S_2}. The photon a undergoes reflection by two plane mirrors, then passes through H_1 and X_1 successively. Afterwards, a Hadamard operation is performed on electronic spin S_2. Then photon a passes through $CPBS_3$, where $|R\rangle$ is transmitted and $|L\rangle$ is reflected, and is subsequently detected by detector D_2. Meanwhile, $|L\rangle$ reflected by $CPBS_2$ passes through a waveform corrector $WFC_2(|i\rangle \rightarrow \frac{1}{2}(r_1-r_0)|i\rangle)$.

If detector D_2 responds, the corresponding state is $|\phi_2\rangle = \frac{1}{4}|L\rangle(r_1-r_0)(r_1+r_0)(\alpha_1\alpha_2|\uparrow\uparrow\rangle+\alpha_1\beta_2|\uparrow\downarrow\rangle)$. If detector D_2 does not respond, a bit-flip operation is performed on electronic spin S_2. Afterwards, photon a passes through H_1, where $CPBS_4$ transmits photon in $|R\rangle$ and reflects photon in $|L\rangle$. Detectors D^+ and D^- detect photon in $|R\rangle$ and $|L\rangle$, respectively. If detector D^- responds, a phase-flip operation is performed on electronic spin S_1, $\sigma_z = |\uparrow\rangle\langle\uparrow| - |\downarrow\rangle\langle\downarrow|$. The electronic spin state will finally evolve to

$$|\varphi\rangle^e_{\text{out}} = \frac{1}{4}(r_1-r_0)^2[\alpha_1|\uparrow\rangle(\alpha_2|\uparrow\rangle+\beta_2|\downarrow\rangle)+\beta_1|\downarrow\rangle(\alpha_2|\downarrow\rangle+\beta_2|\uparrow\rangle)]. \quad (7)$$

The control qubit and target qubit in the final output state are the electronic spins S_1 and S_2, respectively. The evolution of the electronic spins system from the initial state to the final state throughout the entire process is as follows

$$|\psi\rangle^e_{\text{in}} = \alpha_1|\uparrow\rangle(\alpha_2|\uparrow\rangle+\beta_2|\downarrow\rangle)+\beta_1|\downarrow\rangle(\alpha_2|\uparrow\rangle+\beta_2|\downarrow\rangle)$$
$$\overset{\text{CNOT}}{\rightarrow}|\psi\rangle^e_{\text{out}} = \frac{(r_1-r_0)^2}{4}(\alpha_1\alpha_2|\uparrow\uparrow\rangle+\alpha_1\beta_2|\uparrow\downarrow\rangle+\beta_1\alpha_2|\downarrow\downarrow\rangle+\beta_1\beta_2|\downarrow\uparrow\rangle). \quad (8)$$

3. Entanglement purification

Previously, we introduced the construction of an error-rejecting CNOT gate. Here, we will present a scheme for entanglement purification of QD electronic spins based on the error-rejecting CNOT gate, as illustrated in figure 3. The electronic spins in the QD-coupled single-sided optical microcavity systems E_{A_1} E_{B_1} E_{A_2} E_{B_2} are denoted as A_1 B_1 A_2 B_2 respectively. The electronic spins A_1 and A_2 belong to Alice, while the electronic spins B_1 and B_2 belong to Bob. Our scheme consists of two error-rejecting CNOT gates, where the electronic pair A_1B_1 serves as the control qubit and the electronic pair A_2B_2 serves as the target qubit. Suppose the initial state of the mixed entangled state to be purified is represented by a density matrix.

$$\rho = M|\phi^+\rangle\langle\phi^+| + Q|\phi^-\rangle\langle\phi^-| + C|\psi^+\rangle\langle\psi^+| + D|\psi^-\rangle\langle\psi^-|, \quad (9)$$

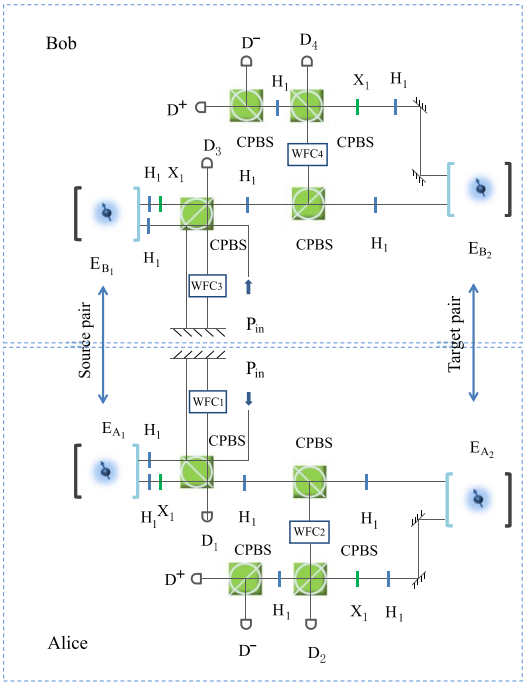

Figure 3. The schematic of QD electron spin entanglement purification using error-reject CNOT gate.

where the coefficients satisfy $M+Q+C+D=1$. M is the fidelity, which represents the probability of the entangled pure state $|\phi^{\pm}\rangle$ in the mixed state. Q, C and D are the corresponding fidelities. $|\phi^{\pm}\rangle$ and $|\psi^{+}\rangle$ are four Bell states, defined as follows $|\phi^{\pm}\rangle=\frac{1}{\sqrt{2}}(|\uparrow\uparrow\rangle\pm|\downarrow\downarrow\rangle),|\psi^{\pm}\rangle=\frac{1}{\sqrt{2}}(|\uparrow\downarrow\rangle\pm|\downarrow\uparrow\rangle)$. Alice and Bob first perform unitary operations U_A and U_B on the control qubit and the target qubit respectively [18]. U_A is $|\uparrow\rangle\rightarrow\frac{1}{\sqrt{2}}(|\uparrow\rangle-i|\downarrow\rangle),|\downarrow\rangle\rightarrow\frac{1}{\sqrt{2}}(|\downarrow\rangle-i|\uparrow\rangle)$. And U_B is $|\uparrow\rangle\rightarrow\frac{1}{\sqrt{2}}(|\uparrow\rangle+i|\downarrow\rangle),|\downarrow\rangle\rightarrow\frac{1}{\sqrt{2}}(|\downarrow\rangle+i|\uparrow\rangle)$. These unitary operations induce the following transformations on the Bell states: $|\phi^{+}\rangle\rightarrow|\phi^{+}\rangle,|\psi^{+}\rangle\rightarrow|\psi^{+}\rangle,$ $|\phi^{-}\rangle\rightarrow|\psi^{-}\rangle,|\psi^{-}\rangle\rightarrow|\phi^{-}\rangle$. After the unitary operations, the density matrix becomes

$$\rho_1=M|\phi^{+}\rangle\langle\phi^{+}|+Q|\psi^{-}\rangle\langle\psi^{-}|+C|\psi^{+}\rangle\langle\psi^{+}|+D|\phi^{-}\rangle\langle\phi^{-}|. \tag{10}$$

Let's first consider the purification of two arbitrary mixed entangled states with identical density matrices. Then the initial state of the system is $\rho_1\otimes\rho_1$. Subsequently, Alice and Bob perform error-rejecting CNOT operations on the electron pairsA_1A_2 and B_1B_2. Let's illustrate with an example:

$$\begin{aligned}|\phi^{+}\rangle_{A_1B_1}\otimes|\phi^{-}\rangle_{A_2B_2}&=\frac{1}{\sqrt{2}}\left(|\uparrow\rangle_{A_1}|\uparrow\rangle_{B_1}+|\downarrow\rangle_{A_1}|\downarrow\rangle_{B_1}\right)\otimes\frac{1}{\sqrt{2}}\left(|\uparrow\rangle_{A_2}|\uparrow\rangle_{B_2}-|\downarrow\rangle_{A_2}|\downarrow\rangle_{B_2}\right)\\&\quad\times\overset{\text{CNOT}}{\rightarrow}\frac{1}{2}\left[|\uparrow\rangle_{A_1}|\uparrow\rangle_{B_1}\left(|\uparrow\rangle_{A_2}|\uparrow\rangle_{B_2}-|\downarrow\rangle_{A_2}|\downarrow\rangle_{B_2}\right)|\downarrow\rangle_{A_1}|\downarrow\rangle_{B_1}\left(|\uparrow\rangle_{A_2}|\uparrow\rangle_{B_2}-|\downarrow\rangle_{A_2}|\downarrow\rangle_{B_2}\right)\right]\\&=\frac{1}{\sqrt{2}}\left(|\uparrow\rangle_{A_1}|\uparrow\rangle_{B_1}-|\downarrow\rangle_{A_1}|\downarrow\rangle_{B_1}\right)\otimes\frac{1}{\sqrt{2}}\left(|\uparrow\rangle_{A_2}|\uparrow\rangle_{B_2}-|\downarrow\rangle_{A_2}|\downarrow\rangle_{B_2}\right)\\&=|\phi^{-}\rangle_{A_1B_1}\otimes|\phi^{-}\rangle_{A_2B_2}.\end{aligned} \tag{11}$$

The error-rejecting CNOT operations for the other Bell bases are provided in the truth table 1. Alice and Bob measure the target qubit electronic pair A_2B_2 in the basis $\{|\uparrow\rangle,|\downarrow\rangle\}$, respectively, and compare the measurement results through a classical channel. If the measurement results are the same, the control qubit electron pair is retained; if the measurement results are different, the control qubit electron pair is discarded. So the density matrix of the retained electron pair is

$$\rho_2=M'|\phi^{+}\rangle\langle\phi^{+}|+Q'|\psi^{-}\rangle\langle\psi^{-}|+C'|\psi^{+}\rangle\langle\psi^{+}|+D'|\phi^{-}\rangle\langle\phi^{-}|, \tag{12}$$

where $M'=\frac{M^2+Q^2}{N},Q'=\frac{2CD}{N},C'=\frac{C^2+D^2}{N},D'=\frac{2MQ}{N},N=(M+Q)^2+(C+D)^2$. Therefore, in the remaining states, the probability of $|\phi^{+}\rangle$ is M'. When $M>\frac{1}{2}$, $M'>M$. In the next round of entanglement

Table 1. Truth table for the error-reject CNOT operation.

Initial state		Final state	
(A_1B_1)	(A_2B_2)	(A_1B_1)	(A_2B_2)
$\left\|\phi^{\pm}\right\rangle$	$\left\|\phi^{+}\right\rangle$	$\left\|\phi^{\pm}\right\rangle$	$\left\|\phi^{+}\right\rangle$
$\left\|\phi^{\pm}\right\rangle$	$\left\|\phi^{-}\right\rangle$	$\left\|\phi^{\mp}\right\rangle$	$\left\|\phi^{-}\right\rangle$
$\left\|\psi^{\pm}\right\rangle$	$\left\|\psi^{+}\right\rangle$	$\left\|\psi^{\pm}\right\rangle$	$\left\|\phi^{+}\right\rangle$
$\left\|\psi^{\pm}\right\rangle$	$\left\|\psi^{-}\right\rangle$	$\left\|\psi^{\mp}\right\rangle$	$\left\|\phi^{-}\right\rangle$
$\left\|\phi^{\pm}\right\rangle$	$\left\|\psi^{+}\right\rangle$	$\left\|\phi^{\pm}\right\rangle$	$\left\|\psi^{+}\right\rangle$
$\left\|\phi^{\pm}\right\rangle$	$\left\|\psi^{-}\right\rangle$	$\left\|\phi^{\mp}\right\rangle$	$\left\|\psi^{-}\right\rangle$
$\left\|\psi^{\pm}\right\rangle$	$\left\|\phi^{+}\right\rangle$	$\left\|\psi^{\pm}\right\rangle$	$\left\|\psi^{+}\right\rangle$
$\left\|\psi^{\pm}\right\rangle$	$\left\|\phi^{-}\right\rangle$	$\left\|\psi^{\mp}\right\rangle$	$\left\|\psi^{-}\right\rangle$

purification, Alice and Bob still need to perform unitary operations U_A and U_B on the control qubit and the target qubit respectively. The density matrix of the retained electron pair is then transformed to:

$$\rho_3 = M'\left|\phi^{+}\right\rangle\left\langle\phi^{+}\right| + Q'\left|\phi^{-}\right\rangle\left\langle\phi^{-}\right| + C'\left|\psi^{+}\right\rangle\left\langle\psi^{+}\right| + D'\left|\psi^{-}\right\rangle\left\langle\psi^{-}\right|. \tag{13}$$

Repeating the entanglement purification process can further improve the fidelity of $|\phi^{+}\rangle$.

If the initial states of the two electron pairs A_1B_1 and A_2B_2 are different, the above process still applies. For example: the initial state of the control qubit electron pair is given by equation (10), while the initial state of the target qubit electron pair is given by equation (12). Similarly, after performing unitary operations and error-rejecting CNOT operations, Alice and Bob measure the target qubit electron pair A_2B_2 in the basis $\{|\uparrow\rangle, |\downarrow\rangle\}$, respectively, and compare the measurement results through classical communication. If the measurement results are the same, the corresponding control qubit electron pair is retained; if the measurement results are different, the corresponding control qubit electron pair is discarded. The density matrix of the retained electron pair is then transformed to:

$$\rho_4 = M''\left|\phi^{+}\right\rangle\left\langle\phi^{+}\right| + Q''\left|\psi^{-}\right\rangle\left\langle\psi^{-}\right| + C''\left|\psi^{+}\right\rangle\left\langle\psi^{+}\right| + D''\left|\phi^{-}\right\rangle\left\langle\phi^{-}\right|. \tag{14}$$

where $M'' = \frac{MM'+QQ'}{N'}, Q'' = \frac{CD+C'D'}{N'}, C'' = \frac{CC'+DD'}{N'}, D'' = \frac{MQ+M'Q'}{N'}, N' = (M+Q)(M'+Q')+(C+D)(C'+D')$. In this case, the relationship between $M\,M'\,M''$ should satisfy: when both M and M' are greater than $\frac{1}{2}$, $M'' > M' > M$. Before purification, unitary operations U_A and U_B need to be applied to the control qubit and the target qubit, respectively. Then the above steps are repeated to further improve the fidelity of $|\phi^{+}\rangle$ in the mixed entangled state. In this way, by repeatedly iterating the above entanglement purification steps, a mixed entangled state with high fidelity can be obtained. After entanglement purification, the fidelity of $|\phi^{+}\rangle$ approaches 1 as the number of iterations increases monotonically. According to $M' = \frac{M^2+Q^2}{N}$, we can see that mathematically, it is a nonlinear mapping equation. When $F > 1/2$, $F = 1$ is a local attractor, so it can only be infinitely approached. In other words, if you want to obtain a state $|\phi^{+}\rangle$ with a fidelity of 1, theoretically, this entanglement purification scheme needs to consume infinite quantum resources. Of course, in practical applications, it is only necessary to perform a finite number of iterations and purifications to make the fidelity of the state $|\phi^{+}\rangle$ approach 1.

In addition, our scheme performs unitary operations U_A and U_B on the source particle pairs and target particles respectively before each round of purification: $|\phi^{+}\rangle \to |\phi^{+}\rangle, |\psi^{+}\rangle \to |\psi^{+}\rangle, |\phi^{-}\rangle \to |\psi^{-}\rangle, |\psi^{-}\rangle \to |\phi^{-}\rangle$. Thereby converting $|\phi^{-}\rangle$ into $|\psi^{-}\rangle$, and achieving a larger-scale reduction in the probability of $|\phi^{-}\rangle$.(The purpose of doing this is that in the traditional scheme, a part of the probability increase of $|\phi^{-}\rangle$ is evenly distributed again to the three non-$|\phi^{+}\rangle$ Bell states, thereby reducing the probability of $|\phi^{-}\rangle$. This will result in some phase errors being converted into bit errors, which will cause the iteration cycle to be slow.) After each round of purification, the entangled source will be applied to the next round of purification after undergoing unitary operations. The above cycle steps are then repeated to further improve the fidelity of $|\phi^{+}\rangle$ in the mixed entangled state.

4. Discussion

QDs are ideal physical entities for realizing quantum information processing. Using spin echo technology, the electronic spin coherence time in QDs can last for more than 3×10^{-3} **ms** [40, 41], and the electronic spin relaxation time can reach the **ms** level [42, 43]. At the same time, the experimental control technology of QDs has developed rapidly, and has achieved the rapid preparation of electronic spin superposition states in QDs [44, 45], rapid manipulation of electronic spins [46–49], and detection of electronic spins [50]. In

addition, it is easier to embed QDs in solid-state cavities which enhances the QD-photon interaction. These advantages make QDs an ideal platform for quantum information processing. Hu *et al* successively constructed a QD-coupled single-sided microcavity system [33] and a QD-coupled double-sided microcavity system, and based on cavity electrodynamics and spin selection rules, obtained the quantum state change rules of the hybrid system after the system was exposed to circularly polarized light [38].

In the process of entanglement purification, it is necessary to measure the electronic spin state on the basis vectors $\{|+\rangle, |-\rangle\}$ and perform Hadamard operation on the electronic spin state. The electronic spin state $|\pm\rangle$ can be converted into $|\uparrow\rangle$ or $|\downarrow\rangle$. These two states can be measured by measuring the helicity of the transmitted (or reflected) photons. At the same time, in our scheme, since right-handed and left-handed polarized light excite the dipole transitions $|\uparrow\rangle \leftrightarrow |\uparrow\downarrow\Uparrow\rangle$ and $|\downarrow\rangle \leftrightarrow |\downarrow\uparrow\Downarrow\rangle$, respectively, it is necessary to support cavity modes with two polarization states of the same frequency. Fortunately, many experiments have provided such technology [51–54].

In addition to being affected by the coefficients g, κ, κ_s, and γ , fidelity is also affected by excitonic damping, including optical damping and spin damping [38, 55]. The reduction in fidelity due to exciton damping can be expressed as $[1 - e^{-\tau/\Gamma}]$, where τ and Γ are the photon lifetime and exciton coherence time in the microcavity, respectively. Optical damping reduces fidelity by less than 10% because the optical coherence time is on the order of hundreds of picoseconds [56–58] , but for In(Ga)As QDs coupled to a microcavity with a quality factor of 10^4–10^5, the intracavity photon lifetime is on the order of tens of picoseconds. The effect of spin damping can be ignored or neglected [59, 60] because the spin decoherence time is on the order of several times the photon lifetime in the microcavity. Fidelity is also affected by imperfect optical transitions caused by mixing of heavy and light holes in the QDs [61]. Imperfect mixing of heavy and light holes can be reduced by choosing the right shape, size, and type of QDs.

5. Conclusion

In this paper, we propose an error-rejecting entanglement purification scheme for QD electronic spins in single-sided optical microcavities. We first utilize QD-coupled single-sided optical microcavity systems to construct an error-rejecting CNOT gate for QD electronic spins. Then, by employing the error-rejecting CNOT gate and unitary operations, we design an error-rejecting entanglement purification scheme for QD electronic spins. This scheme is capable of extracting high-entanglement electronic spin states from low-entanglement mixed states of electronic spins. In QD-coupled single-sided optical microcavity systems, imperfect input-output relations during the interaction between photons and the system can reduce the fidelity of entanglement purification. We utilize the error-rejecting CNOT gate for QD electronic spins to convert the factors that reduce fidelity into detectable operational errors. This approach eliminates the impact of non-ideal interactions on the fidelity of entanglement purification operations. Therefore, the error-rejecting entanglement purification scheme for QD electronic spins has significant practical value in enhancing the entanglement of non-local entanglement systems.

Data availability statement

No new data were created or analyzed in this study.

Acknowledgments

In this paper, all the authors contributed equally to this work. We would like to thank Prof. Fu-Guo Deng, Prof. Bao-Cang Ren and Prof. Chun-Yan Li for useful conversations. This work is supported by the Research Initiation Foundation of Yanshan University (Grant No. 8190456).

References

[1] Kimble H J 2008 *Nature* **453** 1023
[2] Bennett C H, Brassard G, Crépeau C, Jozsa R, Peres A and Wootters W K 1993 *Phys. Rev. Lett.* **70** 1895
[3] Bennett C H and Wiesner S J 1992 *Phys. Rev. Lett.* **69** 2881
[4] Liu X S, Long G L, Tong D M and Li F 2002 *Phys. Rev.* A **65** 022304
[5] Gisin N, Ribordy G, Tittel W and Zbinden H 2002 *Rev. Mod. Phys.* **74** 145
[6] Bužek V and Hillery M 1996 *Phys. Rev.* A **54** 1844
[7] Bennett C H, Brassard G and Mermin N D 1992 *Phys. Rev. Lett.* **68** 557
[8] Li X-H, Deng F-G and Zhou H-Y 2008 *Phys. Rev.* A **78** 022321
[9] Hillery M, Bužek V and Berthiaume A 1999 *Phys. Rev.* A **59** 1829
[10] Long G L and Liu X S 2002 *Phys. Rev.* A **65** 032302

[11] Deng F-G, Long G L and Liu X-S 2003 *Phys. Rev.* A **68** 042317
[12] Briegel H-J, Dür W, Cirac J I and Zoller P 1998 *Phys. Rev. Lett.* **81** 5932
[13] Wang T-J, Song S-Y and Long G L 2012 *Phys. Rev.* A **85** 062311
[14] Li T, Yang G-J and Deng F-G 2016 *Phys. Rev.* A **93** 012302
[15] Dür W, Briegel H-J, Cirac J I and Zoller P 1999 *Phys. Rev.* A **59** 169
[16] Bennett C H, Brassard G, Popescu S, Schumacher B, Smolin J A and Wootters W K 1996 *Phys. Rev. Lett.* **76** 722
[17] Bennett C H, Bernstein H J, Popescu S and Schumacher B 1996 *Phys. Rev.* A **53** 2046
[18] Deutsch D, Ekert A, Jozsa R, Macchiavello C, Popescu S and Sanpera A 1996 *Phys. Rev. Lett.* **77** 2818
[19] Pan J-W, Simon C, Brukner Č and Zeilinger A 2000 *Nature* **410** 1067
[20] Pan J-W, Gasparoni S, Ursin R, Weihs G and Zeilinger A 2003 *Nature* **423** 417
[21] Reichle R, Leibfried D, Knill E, Britton J, Blakestad R B, Jost J D, Langer C, Ozeri R, Seidelin S and Wineland D J 2006 *Nature* **443** 838
[22] Sheng Y-B, Deng F-G and Zhou H-Y 2008 *Phys. Rev.* A **77** 042308
[23] Sheng Y-B and Deng F-G 2010 *Phys. Rev.* A **81** 032307
[24] Sheng Y-B and Deng F-G 2010 *Phys. Rev.* A **82** 044305
[25] Deng F-G 2011 *Phys. Rev.* A **84** 052312
[26] Wang C, Zhang Y and Jin G-s 2011 *Phys. Rev.* A **84** 032307
[27] Lu L-C, Ren B-C, Wang X, Zhang M and Deng F-G 2020 *Ann. Phys., Lpz.* **532** 2000011
[28] Lu L-C, Wang G-Y, Ren B-C, Zhang M and Deng F-G 2020 *Chin. Phys.* B **29** 010305
[29] Cao C, Zhang L, Han Y-H, Yin P-P, Fan L, Duan Y-W and Zhang R 2020 *Opt. Express* **28** 2857
[30] Yin P-P, Cao C, Han Y-H, Fan L and Zhang R 2022 *Quantum Inf. Process.* **21** 1
[31] Young A B *et al* 2011 *Phys. Rev.* A **84** 011803
[32] Hu C Y, Munro W J and Rarity J G 2008 *Phys. Rev.* B **78** 125318
[33] Hu C Y, Young A, O'Brien J L, Munro W J and Rarity J G 2008 *Phys. Rev.* B **78** 085307
[34] Wei H-R and Deng F-G 2014 *Opt. Express* **22** 593
[35] Warburton R J 2013 *Nat. Mater.* **12** 483
[36] Walls D and Milburn G J 2008 *Quantum Optics* (Springer) pp 127–41
[37] Waks E and Vuckovic J 2006 *Phys. Rev.* A **73** 041803
[38] Hu C Y, Munro W J, O'Brien J L and Rarity J G 2009 *Phys. Rev.* B **80** 205326
[39] Bonato C, Haupt F, Oemrawsingh S S R, Gudat J, Ding D, van Exter M P and Bouwmeester D 2010 *Phys. Rev. Lett.* **104** 160503
[40] Petta J R, Johnson A C, Taylor J M, Laird E A, Yacoby A, Lukin M D, Marcus C M, Hanson M P and Gossard A C 2005 *Science* **309** 2180
[41] Greilich A, Yakovlev D R, Shabaev A, Efros A L, Yugova I A, Oulton R, Stavarache V, Reuter D, Wieck A and Bayer M 2006 *Science* **313** 341
[42] Elzerman J, Hanson R, Willems van Beveren L, Witkamp B, Vandersypen L and Kouwenhoven L P 2004 *Nature* **430** 431
[43] Kroutvar M, Ducommun Y, Heiss D, Bichler M, Schuh D, Abstreiter G and Finley J J 2004 *Nature* **432** 81
[44] Atature M, Dreiser J, Badolato A, Hogele A, Karrai K and Imamoglu A 2006 *Science* **312** 551
[45] Atatüre M, Dreiser J, Badolato A and Imamoglu A 2007 *Nat. Phys.* **3** 101
[46] Berezovsky J, Mikkelsen M, Stoltz N, Coldren L and Awschalom D 2008 *Science* **320** 349
[47] Press D, Ladd T D, Zhang B and Yamamoto Y 2008 *Nature* **456** 218
[48] Gupta J A, Knobel R, Samarth N and Awschalom D D 2001 *Science* **292** 2458
[49] Chen P, Piermarocchi C, Sham L J, Gammon D and Steel D G 2004 *Phys. Rev.* B **69** 075320
[50] Hanson R, van Beveren L H W, Vink I T, Elzerman J M, Naber W J M, Koppens F H L, Kouwenhoven L P and Vandersypen L M K 2005 *Phys. Rev. Lett.* **94** 196802
[51] Luxmoore I J, Ahmadi E D, Luxmoore B J, Wasley N A, Tartakovskii A I, Hugues M, Skolnick M S and Fox A M 2012 *Appl. Phys. Lett.* **100** 121116
[52] Bonato C, van Nieuwenburg E, Gudat J, Thon S, Kim H, van Exter M P and Bouwmeester D 2011 *Phys. Rev.* B **84** 075306
[53] Hagemeier J, Bonato C, Truong T-A, Kim H, Beirne G J, Bakker M, van Exter M P, Luo Y, Petroff P and Bouwmeester D 2012 *Opt. Express* **20** 24714
[54] Eto Y, Noguchi A, Zhang P, Ueda M and Kozuma M 2011 *Phys. Rev. Lett.* **106** 160501
[55] Hu C Y and Rarity J G 2011 *Phys. Rev.* B **83** 115303
[56] Borri P, Langbein W, Schneider S, Woggon U, Sellin R L, Ouyang D and Bimberg D 2001 *Phys. Rev. Lett.* **87** 157401
[57] Birkedal D, Leosson K and Hvam J M 2001 *Phys. Rev. Lett.* **87** 227401
[58] Langbein W, Borri P, Woggon U, Stavarache V, Reuter D and Wieck A D 2004 *Phys. Rev.* B **70** 033301
[59] Gerardot B D, Brunner D, Dalgarno P A, Öhberg P, Seidl S, Kroner M, Karrai K, Stoltz N G, Petroff P M and Warburton R J 2008 *Nature* **451** 441
[60] Brunner D, Gerardot B D, Dalgarno P A, Wüst G, Karrai K, Stoltz N G, Petroff P M and Warburton R J 2009 *Science* **325** 70
[61] Bester G, Nair S and Zunger A 2003 *Phys. Rev.* B **67** 161306